Dynamic Modelling of a Fuel Cell and Wind Turbine DC-Linked Power System

B. Francois
Laboratoire d'Electrotechnique et d'Electronique de Puissance de Lille
L2EP , Ecole Centrale de Lille,
Cité Scientifique, BP 48,
59651 Villeneuve d'Ascq Cedex, France
e_mail : bruno.francois@ec-lille.fr

D. Hissel
Laboratoire d'Electrotechnique, Electronique et Systèmes
L2ES, UTBM, UFC,
Rue Thierry Mieg,
90010 Belfort Cedex, France
e_mail : daniel.hissel@utbm.fr

M.T. Iqbal
Faculty of Engineering, MUN,
St. John's, NL, Canada A1B3X5,
Ph: 709 737 8934,
e_mail: tariq@engr.mun.ca

***Abstract*-- An equivalent continuous dynamic model of a fuel cell generator and wind energy conversion system is proposed in this paper. It is shown that this model is interesting for analyzing the dynamic behavior of the system and for designing the control strategy. The proposed global model is simulated with the help of Matlab-Simulink™, by considering a 400 W wind generator and a Proton Exchange Membrane Fuel Cell (PEMFC) generator. This hybrid system is connected to a distribution network which is simulated with the help of the Power System Blockset™ (PSB) toolbox.**

I. Introduction

Many incitations motivate the development of renewable energy based generators [1,2]. Renewable energy based generators have to be exploited much more efficiently in order to make them available. This is the reason why these generators are commonly associated with storage elements to ensure power supply on the long run. Inside these systems the use of power converters enables:

_ the optimization of the energy capture from renewable sources

_ the precise bi-directional transfer of the energy through the storage elements

_ the power conversion at the grid frequency and the control of the active and reactive power generation.

Moreover, a DC bus link gives flexibility of connecting various additional generators and storage elements.

For Wind Energy Conversion Systems (WECS) applications, a possible system consists of using a wind generator which is connected to a flywheel storage element via a dc bus, then the grid connection is performed by a classical inverter with chokes in series [3]. An alternative concept is to exploit hydrogen for long-term energy storage by using an electrolyzer, a hydrogen tank and a fuel cell as shown in figure 1. Recent commercial availability of small proton exchange membrane fuel cell (PEMFC) units makes viable the design of such new hybrid energy systems with energy storage in hydrogen form. Mathematical models of this system are necessary to evaluate various aspects e.g. cost, efficiency, reliability and dynamic response to sudden changes but, before all, design of the control system remains to be optimized.

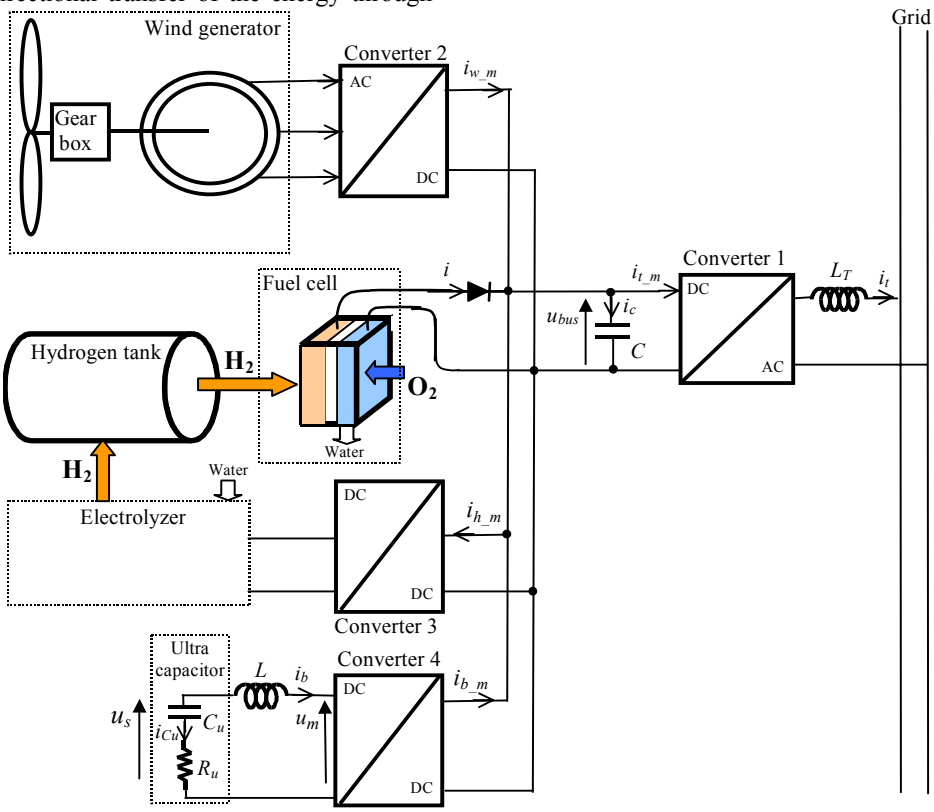

Fig. 1. Hybrid WECS / fuel cell generating system

Let us present you the studied system. The WECS is based on a squirrel cage induction machine connected to a voltage-source power electronic converter. The fuel cell is connected directly to the DC bus. An ultracapacitor and a boost chopper are used to control the dc bus voltage. The connection to the AC grid includes a voltage source converter and chokes to reduce the current ripples.

For simplification, the dynamic modeling of electrolyzer and fuel cell related equipments such as hydrogen storage vessel, compressor, piping, valves etc. were left for a future work.

The aim of this paper is to propose a model of the grid connected fuel cell generator. First the operation principle of a PEMFC is introduced. Then a physics-based-model is presented and is depicted within an associated Causal Ordered Graph (COG). In a third part a model of an ultracapacitor is presented within the model of the dc bus and the grid power converter in part four. Then an Energetic Macro Representation of the entire power system is presented. Finally simulation results highlight voltage and current variations throughout the system.

II. Modelling of a Fuel Cell Stack

A. Operation principle

A PEMFC is an electrochemical device that produces directly water, heat and electricity through the oxido-reduction reaction of hydrogen and oxygen. Hydrogen is located on the anode side and oxygen on the cathode side. An electrolyte membrane between these two compartments allows the exchange of electrical charges (here protons) (Figure 2). A PEMFC is a low temperature fuel cell; indeed, the operating temperature is approximately 80°C. Many approaches have been used to model the PEMFC behavior [5]. Here, a parametric model of PEMFC developed by Amphlett [6,7] using mechanistic approach and based on a Ballard Mark IV single cell is used and now presented.

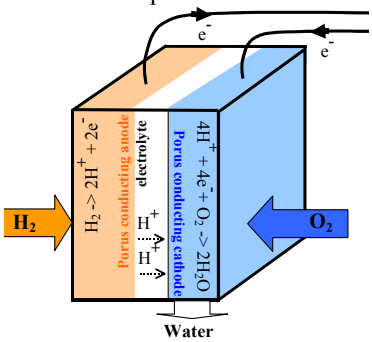

Fig. 2: Schematic of individual fuel cell

B. Fuel cell stack model

The considered fuel cell stack is a H_2/O_2 one and operates with water saturated incoming gases. The maximum electrical output power is considered to be 1kW and it is supposed to be build with 65 single cells. The ideal standard potential (Nernst's potential) of such a single cell (E_o) is 1.229V with liquid water product. The actual cell potential is decreased from its reference potential because of irreversible losses. The thermodynamic potential E is defined via a Nernst equation in expanded form as [7]

$$E_{Nernst} = 1.229 - 0.85\text{x}10^{-3}\,(T - 298.15) + 4.3085\text{x}10^{5}\,.T.(\ln P_{H2} + 0.5\ln P_{O2}) \quad (R1)$$

Where P is the effective pressure in atm. and T is the temperature in Kelvin.

To model the fuel cell stack, an equivalent electrical circuit can be used [8] (fig. 3). The structure and elements of this circuit are now detailed.

The concentration of dissolved oxygen at the gas/liquid interface can be defined by Henry's Law expression of the form [6,7]

$$c_{O2} = \frac{P_{O2}}{5.08\text{x}10^{6}\exp^{-\frac{498}{T}}} \quad (4)$$

The parametric equation for the over-voltage due to activation and the internal resistance developed from the empirical analysis [7] are given as

$$\eta_{act} = -0.9514 + 0.00312\,T - 0.000187\,T\ln(i) + 7.4\text{x}10^{-5}\,T\ln(c_{O2}) \quad (5)$$

$$R_{int} = 0.01605 - 3.5\text{ x }10^{-5}\,T + 8\text{x}10^{-5}\,i \quad (6)$$

In this equation i is the fuel cell current and the activation resistance is determined as:

$$R_a = -\eta_{act}\,\text{x}\frac{1}{i} \quad (7)$$

The combined effect of thermodynamics, mass transport, kinetics, and ohmic resistance determines the output voltage of the cell as defined by [6,7]

$$v_{cell} = E_{Nernst} - v_{act} - v_{Rin} \quad (R2)$$

The ohmic voltage loss in the fuel cell is given by

$$v_{Rint} = Rint\,i \quad (R3)$$

Dynamics of the fuel cell voltage can be modelled, in a very simple way, by an addition of a capacitor C, to the steady state model [8,9]. The effect of double charge layer is modelled by a capacitor C connected in parallel with the activation resistance as shown in Figure 3. A differential equation describes the activation voltage as

$$\frac{dv_{act}}{dt} = \frac{1}{C}i_c \quad (R4)$$

with $i_c = i - i_{Ra}$ (R5) and $i_{Ra} = \frac{1}{Ra}v_{act}$ (R6)

The steady state fuel cell model which is described above

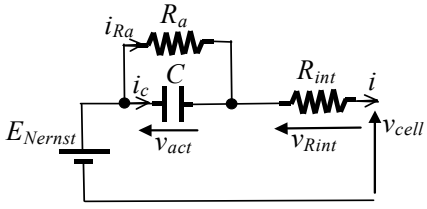

Fig. 3: Equivalent electrical circuit of a fuel cell

indicates the current drawn, cell temperature, H_2 pressure and O_2 pressure will affect the fuel cell output voltage. A drop in the fuel cell voltage can be compensated by an increase in fuel pressure.

C. Anode and cathode model

Amount of hydrogen and oxygen consumed in the fuel cell depends upon the input and output flow rates and the current drawn out of the fuel cell. It also depends upon the volume of electrodes. Assuming that incoming gas flow rates (mole/sec) are known and that the stack is operated in dead-end mode on both sides (except flushes), then gas pressure within fuel cell stack can be determined using the mole conservation principle.

For the fuel cell anode we can write [10]:

$$\frac{dP_{H2}}{dt} = \frac{R}{V_a} T \left(\dot{m}_{H2\ in} - \frac{i}{2F} \right) \qquad (R7)$$

Where, $\dot{m}$ is molar flow rate into the stack compartment,
V_a is anode volume in liters,
R is universal gas constant (0.0821 L-atm/(mol.K),
T is fuel cell temperature (K),
F is Faraday constant (96500 C).

Similarly, an equation for cathode is [10]

$$\frac{dP_{O2}}{dt} = \frac{R}{V_c} T \left(\dot{m}_{O2\ in} - \frac{i}{4F} \right) \qquad (R8)$$

Where V_c is the cathode volume in litres.
Both anode and cathode volumes were assumed as 2L.
A Causal Ordered Graph (see the annexe for more details) of all used mathematical equations is shown on figure 4.

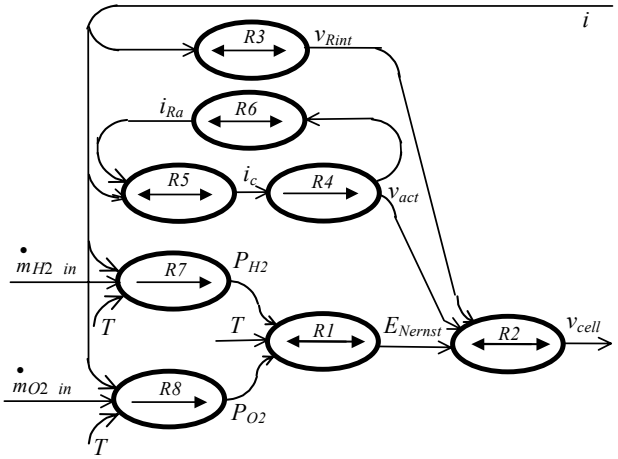

Fig. 4: Causal Ordered Graph of one fuel cell model

E. Temperature estimation

The overall thermal energy balance in an air-cooled fuel cell stack can be expressed as [11]:

Internal heat generation =

Thermal energy stored + Heat losses to ambient

Fuel cell current and internal resistance can be used to calculate internal heat losses as:

$$\text{Internal heat generation} = i^2 (R_a + R_{int}).65$$

where 65 is the number of single cells in series.

Thermal energy stored in fuel cell can be given as:

$$\text{Thermal energy stored} = C_t dT/dt$$

Where C_t is the heat capacity of fuel cell (assumed as 10000 J/°C) and T is the fuel cell temperature.

$$\text{Heat loss to ambient} = (T-T_a)/R_t$$

Substituting equation 15 to 17 in equation 14 and simplifying results in

$$dT/dt = 65.\ i^2 (R_a + R_{int})/C_t - (T - T_a)/R_t /C_t$$

Ambient temperature, T_a was assumed as 25°C and R_t = 0.04 °C/W.

D. Modelling of the stack

The fuel cell system consists of a stack of 65 similar single cells which are connected in series. Therefore the total stack voltage is given by:

$$v_{stack} = 65\ v_{cell} \qquad (R9)$$

$$v_{R\_stack} = v_{stack} - v_s \qquad (R10)$$

$$i = \frac{1}{R_{stack}} v_{R\_stack} \qquad (R11)$$

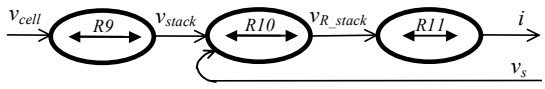

Fig. 5: Causal Ordered Graph of a stack

III. MODELLING OF THE ULTRA CAPACITOR

A. Modelling of the component

Ultra-capacitors are used in power applications requiring a short duration peak power. Such an ultra-capacitor module can be connected in parallel with the fuel cell to reduce its voltage variation due to sudden load changes. Four Maxwell 435F, 14V ultra-capacitor modules were selected. Selected ultra-capacitor module has a series resistance of 4mΩ and leakage current of 10mA. For simulation purpose the leakage current of the ultra-capacitor was assumed constant.

Current drawn by the cooling fan of ultracapacitor was neglected. This ultracapacitor has been modelled by using a total capacitor of 108.75F (Cu) in series with a resistor of 16mΩ (Ru) (fig. 6).

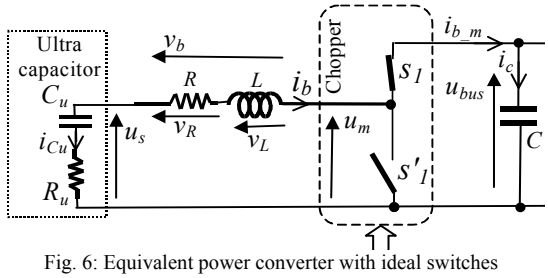

Fig. 6: Equivalent power converter with ideal switches

This ultra-capacitor is then modelled with following equations:

$$i_{Cu} = -i_b \quad (R12) \qquad \frac{du_{Cu}}{dt} = \frac{1}{Cu} i_{Cu} \quad (R13)$$

$$u_{Ru} = Ru\, i_{Cu} \quad (R14) \qquad u_S = u_{Ru} + u_{Cu} \quad (R15)$$

The corresponding Causal Ordered graph is depicted on fig.7.

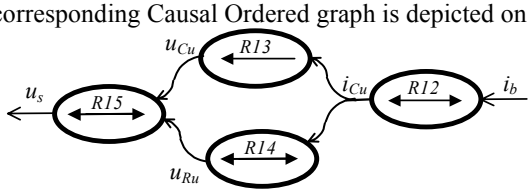

Fig. 7: Causal Ordered Graph of the ultracapacitor

B. Modelling of the choke

The capacitor current is obtained by integration of the voltage as :

$$\frac{di_b}{dt} = \frac{1}{L}.v_L \quad \text{or} \quad i_b(t) = \frac{1}{L}.\int_t^{t+\Delta t} v_L\, dt + i_b(to) \quad (R16)$$

A voltage appears across the resistor as:

$$v_R = R\, .i_b \quad (R17)$$

Then the voltage across the inductor results from this voltage and the choke voltage as:

$$v_L = v_b - v_R \quad (R18)$$

In a same way the choke voltage results from the grid voltage and the modulated voltage as:

$$v_b = u_s - u_m \quad (R19)$$

The corresponding COG is represented on fig. 8.

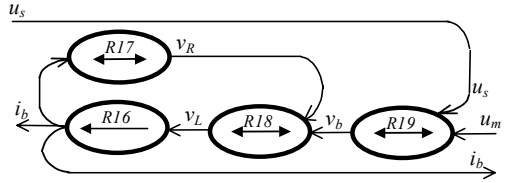

Fig. 8: Causal Ordered Graph of the choke

C. Modelling of the boost chopper

In order to take into account switching harmonics, which are generated in currents, semi conductors in power converters are assumed ideal: no power losses and instantaneous switching. In this case, the chopper model is equivalent to a set of two ideal switches [12]. If one switch conducts then we quantify this state as a switching function (s_x) whose value is equal to 1. Otherwise the corresponding switching function is equal to *0.* This switching function is the theoretical state of the switch [13]. At any time, only one switch in a vertical switching cell is in on state. Then the following constraint must be followed :

$$s_x = s'_x$$

And so there exists only two configurations (fig. 9). The resulting modulated voltage from the chopper is then expressed by :

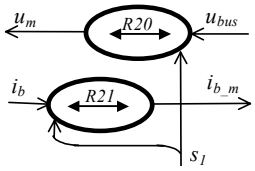

s'_1	s_1	u_m	ib_m
1	0	0	0
0	1	u_{bus}	i_b

Fig. 9: Causal Ordered Graph of the chopper

$$u_m = s_1 . u_{bus} \quad (R20)$$

The modulated current from the chopper is expressed as :

$$i_{b\_m} = s_1 .\, i_b \quad (R21)$$

IV. MODELLING OF THE ELECTRICAL CHAIN

A. Modelling of the dc bus

The capacitor voltage from the dc bus is obtained by integration of the total capacitor current:

$$\frac{du_{bus}}{dt} = \frac{1}{C}.i_c \quad (R22)$$

This capacitor current results from all collected currents:

$$i_c = i_{b\_m} + i + i_{w\_m} - i_{t\_m} - i_{h\_m} \quad (R23)$$

The corresponding COG is represented on fig. 10.

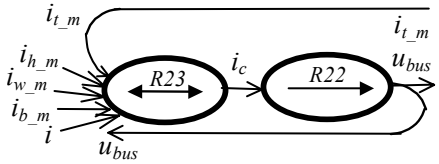

Fig. 10: Causal Ordered Graph of the dc bus

B. Modelling of the inverter and the ac filter

By considering again two circuits of two ideal switches we get only four possible states (fig. 11). Then the modulated voltage from the single phase inverter is expressed by :

$$vm = m\, .u_{bus} \quad (R24)$$

The modulation function (m) is a three level function which is linked to switching functions as :

$$m = s_2 - s_3 \quad (R25)$$

In a same way the modulated current is expressed as:

$$i_{t\_m} = m.\, i \quad (R26)$$

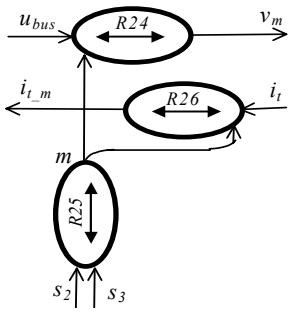

s_2	s_3	v_m	i_{t_m}	m
0	0	0	0	0
0	1	$-u_{bus}$	$-i_t$	-1
1	0	u_{bus}	i_t	1
1	1	0	0	0

Fig. 11: Causal Ordered Graph of the dc bus

V. MACRO MODELLING OF THE ENTIRE SYSTEM

For the wind generator a power model with the wind speed as input has been used [14]. Each preceding COG of electrical components can be viewed as an input-output system which has been represented as squares with an internal diagonal only if they have a storage element (inductance, capacitor). The global model of the power system is then obtained by cascading all component models (fig. 12).

VI. SIMULATION RESULTS

This power system has been simulated with a particular wind profile, which has been forced to a null value at the end (fig. 13).

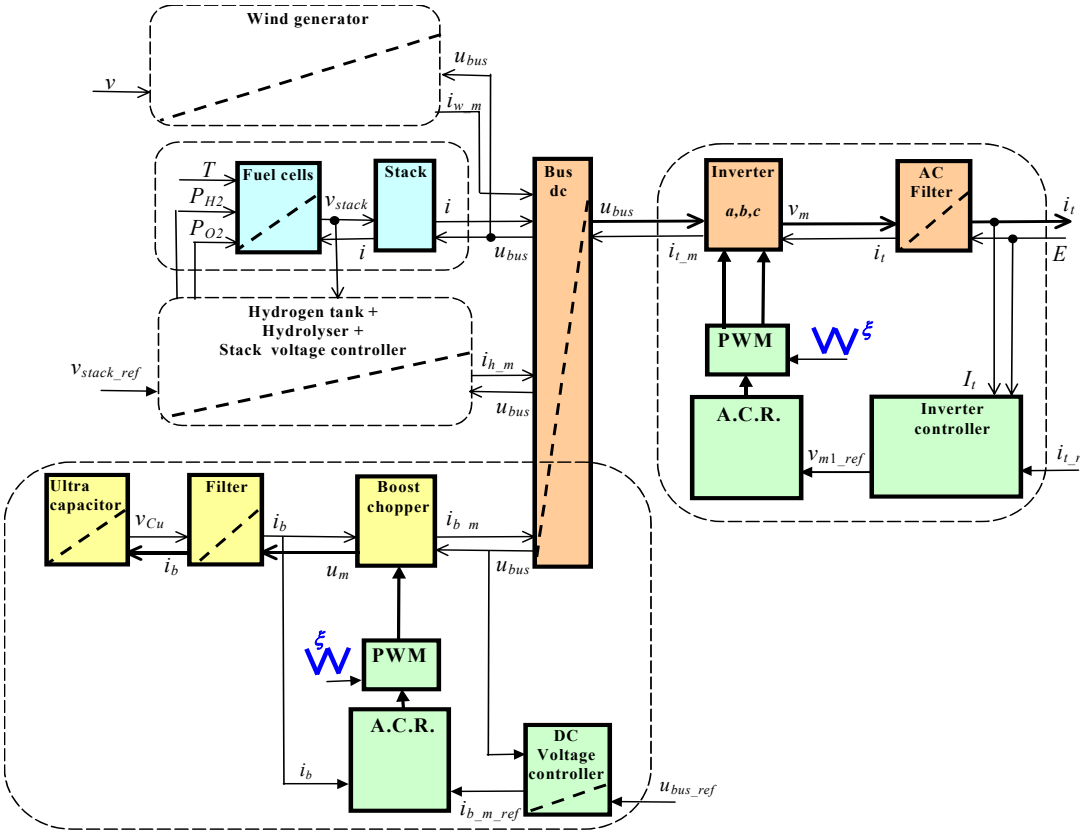

Fig. 12: Macro representation of the system

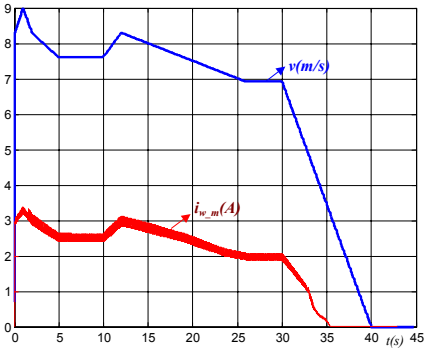

FIG. 13: Wind speed (v) and generated current (i_{w_m})

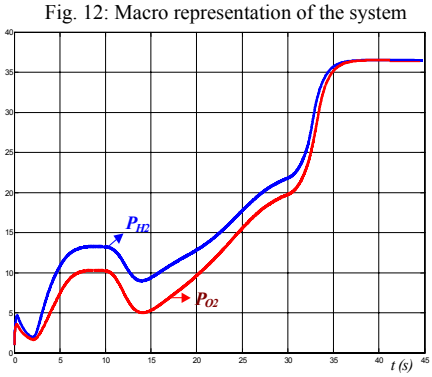

FIG. 14: Hydrogene and Oxygen pressure

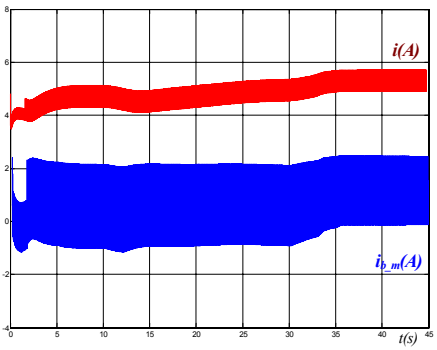

FIG. 15: Fuel cell current (i) and ultra cap current (i_{b_m})

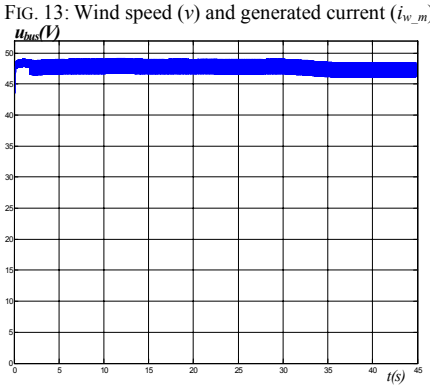

FIG. 16: DC bus voltage (u_{bu})

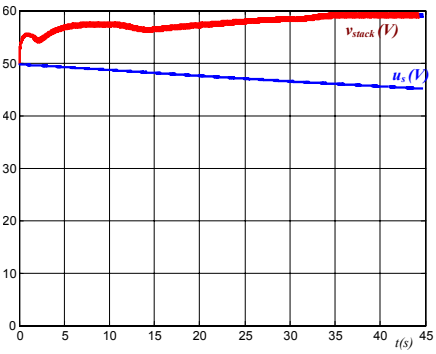

FIG. 17: Fuel cell stack voltage and ultra cap voltage

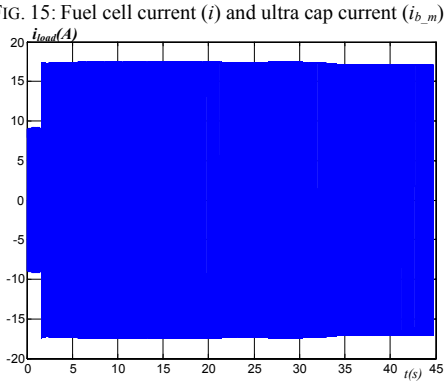

FIG. 18: AC load current

We can see that the generated wind current is nearly proportional to the wind speed and that the wind generator is stopped for wind speed under 3 m/s.

At t =2s, the load has been doubled. In consequence we see that hydrogen and oxygen pressures are automatically increased (fig. 14) in order to increase the fuel cell current (fig. 15). Thanks to the ultra capacitor the modulated current (i_{b_m}) regulates fast transients in order to stabilize the common dc bus voltage.

At t =35s, the wind generator do not produce power and so a constant evolution is observed onto pressures (fig. 14), currents (fig. 15) and the stack voltage (fig. 17). This model demonstrates that the load can be fed at constant power with the fuel cell unless the lack of renewable power.

It must be noted that oscillations of the fuel cell current can be significantly reduced by using a choke or by a more precise timing decoupling of the dc bus voltage control.

VII. CONCLUSION

In this paper we have presented a detailed modeling of a fuel cell by using a particular graphical representation (COG). This mathematical model has been inserted in a more complex power system whose the dc bus is used as a link for connecting various generators and storage elements. In a second step a more detailed modeling of the electrolyzer within the hydrogen tank has to be developed. Then future research ways will be oriented to the design of an integrated power supervision system of this hybrid power generation system.

VIII. REFERENCES

1. R. Mukand Patel, *Wind and solar power systems*, CRC Press, 1999

2. F. Giraud, Z.M. Salameh, "Steady-state performance of a grid connected rooftop Hybrid wind-photovoltaic power system with battery storage", *IEEE Trans on Energy Conversion,* Vol 16, March 2001, pp1-7

3. L. Leclercq, C. Saudemont, B. Robyns, G. Cimuca, M. Radulescu, "Flywheel energy storage system to improve te integration of wind generators into a network", Electromotion journal, No10, 2003, p.641-646

4. EG&G Services Inc., *Fuel Cell Handbook*, 5th edition, (DE-AM26-99FT40575), U.S. Department of Energy, October 2000.

5. Rowe A, Li X., "Mathematical modeling of proton exchange membrane fuel cells", Journal of power sources, Vol. 102, pp82-96, 2001.

6. Mann R F, Amphlett J C, Hooper M, Jensen H M, Peppley B A, Roberge P R., "Development and application of a generalized steady state electrochemical model of a PEM fuel cell", Journal of power sources. Vol. 86 pp 173-180, 2000.

7. Amphlett J C, Baumert R M, Mann R F, Peppley B A, Roberge P R and Harries T J., "Performance modelling of the Ballard mark-IV solid polymer electrolyte fuel cell", Journal of electrochemical society. Vol. 142. No.1 pp 9-15. 1995

8. Larminie J, Dicks A., *Fuel cell systems explained*, John Wiley and sons. England 2001.

9. Bertoni L., Gualous H., Hissel D., Bouquain D., Péra M.C., Kauffmann J.M., "A new design for an auxiliary power unit (APU) by associating supercapacitors and a proton exchange membrane fuel cell", MAGLEV 2002, Lausanne, Suisse, 2002.

10. Gemmen R.S, "Analysis for the Effect of Inverter Ripple Current on Fuel Cell Operating Conditions", 2001 ASME International Mechanical Engineering Congress and Expositions, November 11-16, 2001, NY.

11. Amphlett J. C., Mann R. F., Peppley B. A., Roberge P. R., Rodrigues A. and Salvador J. P.A, "Model predicting transient responses of proton exchange membrane fuel cells", J. Power Sources 61 (1-2), 183-188. (1996)

12. B. Francois, J.P. Cambronne, J.P. Hautier, " A New Approach for Synthesizing Logic Connection Controller in Power Converters ", 6th European Conference on Power Electronics and Applications: EPE'95, p. 693-698, vol.3, Sevilla, Spain, September 17-21 1995

13. B. Francois, J.P. Hautier, " Pulse Position and Pulse Width Modulation of Electrical Power Conversions : Application to a Three-Phase Voltage-Fed Inverter ", 3rd International Symposium on Advanced Electromechanical Motion Systems : ELECTROMOTION 1999, Vol.2, p.653-658, Patras, Greece, July 8-9,1999

14. M. J. Khan, M. T. Iqbal, "Dynamic Modelling and Simulation of a Small Wind Fuel Celll Hybrid Energy System", SESCI 2003 Conference, Ontario, Canada, 2003

15. X. Guillaud, B. Francois, "A causal method for the modelling of static converter and the control design: Application to a Voltage Source Converter", EPE 2003, September 2003, CD, Toulouse, France

16.X. Guillaud, P. Degobert, J.P. Hautier, "Modeling Control and Causality : The Causal Ordering Graph", 16th IMACS Control Engineering, Lausanne 2000

IX. ANNEXE: FONDATION OF THE COG

The Causal Ordered Graph (COG) is a graphical representation of mathematical equations, which are used to model a system [15], [16]. Balloons with inside the equation number represent modeling relations. A time-dependent relation:

$$y(t) = Ra(x(t), t)$$

will be characterized by an unidirectional arrow in the balloon. Dynamics of physical systems are classically described by differential equations:

$$\frac{dy(t)}{dt} = a.x(t) + b \cdot \qquad (Ra)$$

This first order differential equation is typically a time-dependent relation and will be represented as in fig. A.1. Moreover the mathematical property of differential equations specifies that this equation type have an input-output orientation. Meanwhile for equation *(Ra)* the variable *x(t)* must be the input and *y(t)* must be the output. Physically one says that the element (which is described by this time-dependent relation) has an internal causality orientation.

A static relation has no time dependence. It will be depicted as a balloon with a bi-directional arrow (fig .A.2). Physically one says that the corresponding element (which is described by this static relation) has an external causality orientation. If the variable x is externally set then we get:

$$y(t) = Rb(x(t)) \qquad (Rb)$$

Fig. A: COG of dynamic and static relations